Channel-Lining Residues in the M3 Membrane-Spanning Segment of the Cystic Fibrosis Transmembrane Conductance Regulator†

Myles H. Akabas*

Center for Molecular Recognition and Departments of Physiology & Cellular Biophysics and Medicine, College of Physicians and Surgeons, Columbia University, 630 West 168th Street, New York, New York 10032

Received April 29, 1998; Revised Manuscript Received June 26, 1998

ABSTRACT: The cystic fibrosis transmembrane conductance regulator (CFTR) forms a chloride-selective channel. Residues from the 12 putative membrane-spanning segments form at least part of the channel lining. We need to identify the channel-lining residues in order to understand the structural basis for the channel's functional properties. Using the substituted-cysteine-accessibility method we mutated to cysteine, one at a time, 24 consecutive residues (Asp192−Ile215) in the M3 membrane-spanning segment. Cysteines substituted for His199, Phe200, Trp202, Ile203, Pro205, Gln207, Leu211, and Leu214 reacted with charged, sulfhydryl-specific reagents that are derivatives of methanethiosulfonate (MTS). We infer that these residues are on the water-accessible surface of the protein and probably form a portion of the channel lining. When plotted on an α-helical wheel the exposed residues from Gln207 to Leu214 lie within an arc of 60°; the exposed residues in the cytoplasmic half (His199−Ile203) lie within an arc of 160°. We infer that the secondary structures of the extracellular and cytoplasmic halves of M3 are α-helical and that Pro205, in the middle of the M3 segment, may bend the M3 segment, moving the cytoplasmic end of the segment in toward the central axis of the channel. The bend in the M3 segment may help to narrow the channel lumen near the cytoplasmic end. In addition, unlike full-length CFTR, the current induced by the deletion construct, Δ259, is inhibited by the MTS reagents, implying that the channel structure of Δ259 is different than the channel structure of wild-type CFTR.

The cystic fibrosis transmembrane conductance regulator (CFTR)[1] is a member of the gene superfamily of ATP-binding cassette membrane transporters (*1*). CFTR forms an ion channel that is involved in chloride transport in a variety of epithelia and other cells (*2, 3*). CFTR also appears to regulate the activity of other ion channels, such as the outward-rectifying chloride channel (*4*−*6*), the amiloride-sensitive sodium channel (*7*), and perhaps an ATP conduction pathway (*8*). Defects in the gene encoding CFTR cause cystic fibrosis (CF), the most common lethal genetic disease in Caucasians. Overstimulation of CFTR in intestinal crypt cells as a consequence of the actions of various enterotoxins results in secretory diarrhea, a major cause of infant mortality and morbidity (*9, 10*).

The regulation and functions of CFTR have been extensively studied. CFTR forms a small conductance, multiple-ion occupancy chloride channel with a linear current−voltage relationship (*2, 3, 11*). Phosphorylation of CFTR by cAMP- or cGMP-dependent protein kinase and by protein kinase C is a necessary step in the activation process (*10, 12*−*16*). Channel gating involves the binding and hydrolysis of ATP by phosphorylated CFTR (*3, 17*−*20*).

On the basis of hydrophobicity analysis and homology with the ATP-binding cassette transporter gene superfamily, CFTR is predicted to consist of a tandem repeat of six membrane-spanning segments and a nucleotide-binding fold (NBF); the two halves are joined by a cytoplasmic regulatory domain (Figure 1A) (*1*). Experimental evidence supports the predicted transmembrane topology. The extracellular location of the predicted extracellular loops is supported by antibody binding to an epitope in the M1−M2 loop (*21*), antibody binding to an epitope inserted into the M7−M8 loop (*22*), the presence of the endogenous glycosylation sites within the M7−M8 loop (*23*), and glycosylation site insertion (*23*). The cytoplasmic location of the NBFs is supported by the requirement for cytoplasmic ATP to activate the channels in patch clamp studies (*2, 17, 18, 24*). The cytoplasmic location of the R-domain is indicated by its phosphorylation in vivo (*13, 15, 25, 26*).

The channel is presumably lined, at least in part, by residues from among the 12 membrane-spanning segments. Among the residues lining the channel are likely to be the residues that are the major determinants of the functional properties of the CFTR channel. Mutation of residues in the membrane-spanning segments alters the functional properties of the channel. Mutation of some of the charged residues in the membrane-spanning segments altered halide

† This work was supported in part by research grants from the National Institutes of Health (DK51794 and NS30808) and the Cystic Fibrosis Foundation. M.H.A. is the recipient of an Established Scientist Award from the New York City Affiliate of the American Heart Association.

* To whom correspondence should be addressed at the Center for Molecular Recognition, Columbia University, 630 West 168th St., Box 7, New York, NY 10032. Tel 212-305-3974; Fax 212-305-5594; Email ma14@columbia.edu.

[1] Abbreviations: CF, cystic fibrosis; CFTR, cystic fibrosis transmembrane conductance regulator; cpt-cAMP, 8-[(4-chlorophenyl)thio]-adenosine cyclic monophosphate; IBMX, 3-isobutyl-1-methylxanthine MTS, methanethiosulfonate; $MTSEA^+$, 2-ammonioethyl methanethiosulfonate; $MTSES^-$, 2-sulfoethyl methanethiosulfonate; $MTSET^+$, 2-(trimethylammonio)ethyl methanethiosulfonate; NBF, nucleotide-binding fold; SCAM, substituted-cysteine-accessibility method.

S0006-2960(98)00969-6 CCC: $15.00
Published on Web 08/14/1998

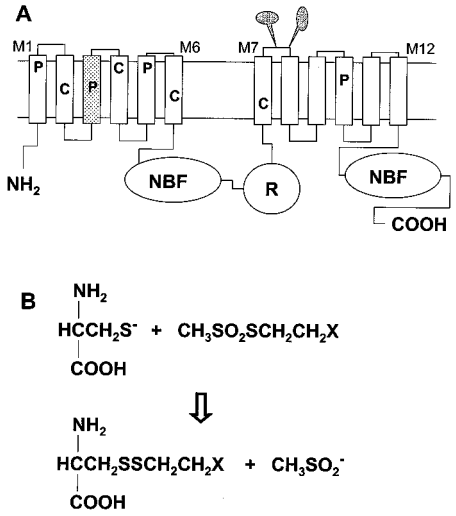

FIGURE 1: Transmembrane topology of CFTR and reaction of the MTS reagents with cysteine. (A) Transmembrane topology of CFTR. In the membrane-spanning segments, C indicates the position of the endogenous cysteine residues and P indicates the position of proline residues; the M3 segment is stippled. The glycosylation sites are indicated by the gray balloons on the fourth extracellular loop. NBF, nucleotide-binding fold; R, R-domain. (B) Reaction of cysteine with an MTS reagent. Top line, reactants; cysteine is shown as an ionized thiolate anion because this form reacts 5×10^9 times faster with the MTS reagents than the un-ionized thiol (*42*). The X is the charge group: SO_3^- for $MTSES^-$; NH_3^+ for $MTSEA^+$; $N(CH_3)_3^+$ for $MTSET^+$.

permeability and/or conductance ratios (*27*). Mutation of Arg347, in the M6 membrane-spanning segment, altered multiple ion occupancy (*28*), and mutations in the M6 and M12 segments altered channel block by diphenylamine-2-carboxylate (*29*). Several mutations associated with mild clinical disease and mutation of a proline residue showed altered single-channel properties (*30, 31*). Furthermore, the assembly of CFTR involves interactions between membrane-spanning segments in the two halves of CFTR (*32*). Thus, to understand the structural bases for the functional properties of the channel, the residues lining the channel must be identified and the secondary and tertiary structure of the channel lining segments must be determined.

There have been several approaches to structural studies of the membrane-spanning segments. By use of spectroscopic techniques on synthetic peptides corresponding to the sequences of the M1−M6 membrane-spanning segments, the secondary structure of the peptides was shown to be largely α-helical in liposomes and in detergent micelles (*33*). Using the substituted-cysteine-accessibility method (*34*), we have systematically identified residues in the M1 and M6 membrane-spanning segments that are on the water-accessible surface of the protein (*35, 36*): Three residues out of nine tested in the middle of the M1 membrane-spanning segment and 11 residues in and flanking the M6 segment were on the water-accessible surface of CFTR. We inferred that most of the corresponding wild-type residues are exposed in the channel lumen (*35, 36*). In general, the periodicity of the accessible residues is consistent with an α-helical secondary structure for the membrane-spanning segments. Thus, an outline of the structure of the channel-forming domains is beginning to emerge through the determination of the secondary structure of the membrane-spanning segments and through the identification of the residues that line the channel.

We have now applied the substituted-cysteine-accessibility method to the residues in the M3 membrane-spanning segment. In this method, consecutive residues in putative channel-lining, membrane-spanning segments are mutated to cysteine, one at a time. Each cysteine-substitution mutant is expressed in *Xenopus* oocytes, and if it has near-normal function, the susceptibility of the engineered cysteine to chemical modification by charged, sulfhydryl-specific reagents, derivatives of methanethiosulfonate (MTS), is determined. We assume that only engineered-cysteine residues on the water-accessible surface of the protein will be accessible for modification by the sulfhydryl reagents. In a protein whose X-ray crystal structure is known, the aspartate chemotaxis receptor, the reactivity of engineered cysteine residues was shown to correlate directly with the water accessibility of the corresponding wild-type residue (*37*). We infer that for a cysteine-substitution mutant whose conduction is irreversibly altered by the sulfhydryl-specific reagents, the side chain of the corresponding wild-type residue is on the water-accessible surface and, thus, may line the channel.

Application of the MTS reagents from the extracellular bath has no effect on wild-type CFTR-induced currents. This indicates that none of the 18 endogenous cysteines, four in membrane-spanning segments and 14 in putative cytoplasmic domains, are accessible to MTS reagents applied extracellularly (*35*). One cysteine in the R-domain, Cys832, is accessible to react with *N*-ethylmaleimide applied from the cytoplasmic bath; reaction at this position stimulates channel activity (*38*).

We now report the identification of eight water-accessible residues in and flanking the M3 membrane-spanning segment. In addition, we show that the current induced by the deletion construct, Δ259, is inhibited by the MTS reagents applied extracellularly.

EXPERIMENTAL PROCEDURES

Oligonucleotide-Mediated Mutagenesis. The cDNA encoding human CFTR in the pBluescript KS(−) vector (CFTR-pBS) was obtained from Dr. A. E. Smith (Genzyme). The altered sites mutagenesis procedure (Promega) was used to substitute cysteine, one at a time, for 24 consecutive residues, Asp192−Ile215, as previously described (*35*). Mutations were identified by restriction digestion and confirmed by DNA sequencing.

Deletion Construct Δ259. The deletion construct that removes the first 259 residues of CFTR, Δ259-pBQ4.7, was obtained from Drs. W. Guggino (Johns Hopkins University) and E. Schwiebert (University of Alabama, Birmingham) (*39*). To generate template for in vitro mRNA transcription, Δ259-pBQ4.7 was linearized with *Eco*RV. Messenger RNA was synthesized with T7 RNA polymerase.

Preparation of mRNA and Oocytes. For in vitro mRNA transcription, CFTR-pBS was linearized with *Sma*I. Messenger RNA was synthesized, and oocytes from *Xenopus laevis* were prepared and maintained as described previously (*34*). One day after the oocytes were harvested, they were injected with 50 nL of mRNA (200 pg/nL). Experiments were performed 1−6 days after mRNA injection.

Sulfhydryl Reagents. The sulfhydryl reagents we have used are derivatives of methanethiosulfonate (MTS): one negatively charged, 2-sulfoethyl methanethiosulfonate

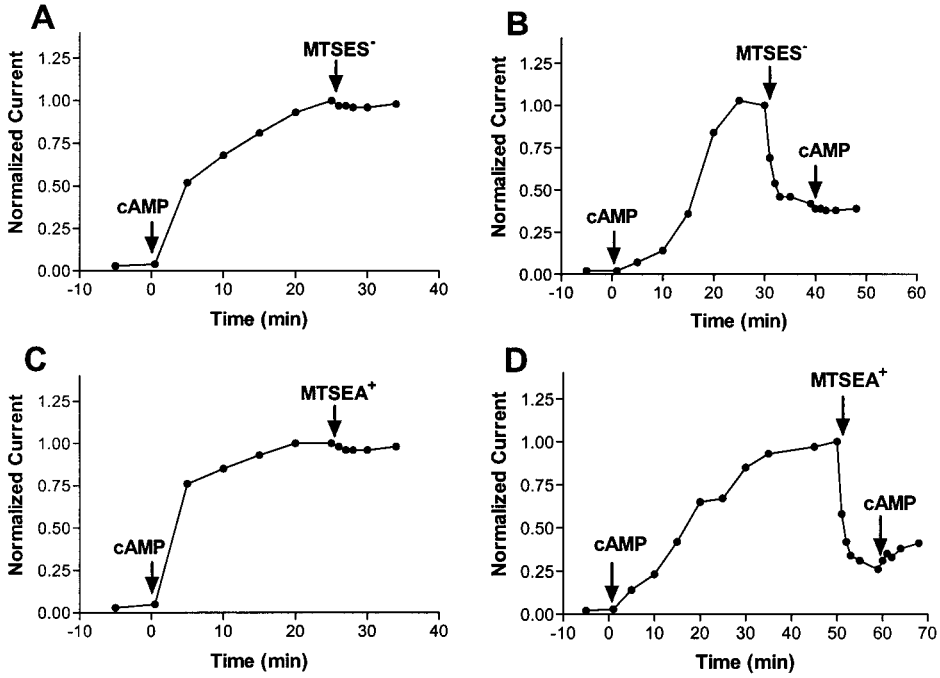

FIGURE 2: MTS reagents do not inhibit currents induced by wild-type CFTR but they do inhibit currents induced by the L211C mutant. Normalized current at −100 mV recorded from individual oocytes expressing wild-type CFTR (A and C) and the L211C mutant (B and D). At the arrows marked cAMP, forskolin, IBMX, and cpt-cAMP were added to the bath. In panels A and B at the arrow marked $MTSES^-$, 10 mM $MTSES^-$ was added to the bath in the continued presence of the protein kinase A activating reagents. In panels C and D at the arrow marked $MTSEA^+$, 2.5 mM $MTSEA^+$ was added to the bath in the continued presence of the protein kinase A activating reagents. The currents were normalized to the value immediately preceding the addition of the MTS reagent: (A) 3286 nA, (B) 5566 nA, (C) 12 061 nA, and (D) 8691 nA. Note that in panels B and D the current does not recover following washout of the MTS reagent, indicating that the effect of the reagent is irreversible.

($MTSES^-$, $CH_3SO_2SCH_2CH_2SO_3^-$) and two positively charged, 2-ammonioethyl methanethiosulfonate ($MTSEA^+$, $CH_3SO_2SCH_2CH_2NH_3^+$), and 2-(trimethylammonio(ethyl methanethiosulfonate [$MTSET^+$, $CH_3SO_2SCH_2CH_2N(CH_3)_3^+$] (*34*, *40*). The MTS reagents add $-SCH_2CH_2X$ to free sulfhydryls to form a mixed disulfide, where X is SO_3^- for $MTSES^-$, NH_3^+ for $MTSEA^+$, and $N(CH_3)_3^+$ for $MTSET^+$ (Figure 1B). The MTS reagents were synthesized as described (*40*) or obtained from Toronto Research Chemicals, Inc. (North York, Ontario, Canada).

Electrophysiology. CFTR-induced currents were recorded from individual oocytes under two-electrode voltage clamp as described previously (*35*). Electrodes were filled with 3 M KCl and had a resistance of less than 2 MΩ. The ground electrode was connected to the bath by a 3 M KCl/agar bridge. During experiments, the oocytes were maintained in Ca^{2+}-free frog Ringer solution (115 mM NaCl, 2.5 mM KCl, 1.8 mM $MgCl_2$, and 10 mM HEPES, pH 7.5 with NaOH) at room temperature. The holding potential was maintained at −10 mV. The CFTR-induced conductance was determined from the current induced by periodically ramping the holding potential from −120 to +50 mV over 1.7 s. From the resulting current−voltage relationship we determined the magnitude of the CFTR-induced current at −100 mV and the reversal potential. The conductance was measured in this manner to avoid changing the intracellular Cl^- concentration during the course of the experiments because Cl^- is passively distributed in *Xenopus* oocytes.

Experimental Protocol. We tested the susceptibility of wild-type and mutant CFTR to the MTS reagents using the following protocol (Figure 2). The CFTR current was activated by application of 200 μM 8-[(4-chlorophenyl)thio]-adenosine cyclic monophosphate (cpt-cAMP), 1 mM 3-isobutyl-1-methylxanthine (IBMX), and 20 μM forskolin in Ca^{2+}-free frog Ringer solution to the extracellular bath to elevate intracellular cAMP and activate protein kinase A (these reagents are subsequently referred to as the protein kinase A activating reagents). When the CFTR-induced current approached a plateau (15−60 min later), i.e., when the rate of increase of the current was less than 2%/min over a 5 min period, the MTS reagents were applied in the extracellular bath in the presence of the protein kinase A activating reagents for 8 min. The sulfhydryl reagents were applied to the oocytes at the following concentrations: 10 mM $MTSES^-$, 2.5 mM $MTSEA^+$, or 1 mM $MTSET^+$, in order to compensate for differences in their reactivities with nonprotein sulfhydryls in solution (*34*, *40*). To determine whether the effects of the MTS reagents were irreversible, the MTS reagents were removed by washing with a solution containing the protein kinase A activating reagents. To compare the effects of MTS reagents in different oocytes, the currents recorded from each oocyte were normalized by the current that was measured immediately before the MTS reagents were applied (Figure 2).

Statistics. Data are presented as the means ± SEM. Significance was determined by one-way analysis of variance with the least significant difference method ($P < 0.05$) using the SPSS-PC statistics package (SPSS, Inc., Chicago, IL).

RESULTS

Characterization of the Mutants. Cysteine was substituted at 24 consecutive positions (Asp192−Ile215), one at a time. All of the mutants expressed cAMP-activated currents in

Xenopus oocytes within 1 day after injection of mRNA. The baseline conductance of the oocytes was generally less than 2.5 μS. The average cAMP-stimulated CFTR conductance for the cysteine-substitution mutants ranged between 49 μS for P205C and 142 μS for the A198C mutant (Figure 3A); for wild type the average conductance was 108 μS. The cAMP-stimulated current reached a plateau within 22 min in oocytes expressing wild-type CFTR. For the cysteine-substitution mutants the time to reach the plateau ranged from 19 min for the L197C mutant to 57 min for the I203C mutant (Figure 3B). It is interesting to note that all of the cysteine-substitution mutants that were not affected by the MTS reagents except D192C and E193C reached the plateau current in less than 30 min. In contrast, the MTS-reactive mutants all took longer than 30 min to reach the plateau current (Figure 3C). In general the plateau conductance of the MTS-susceptible mutants was lower than that of the other mutants (Figure 3C); at present we have no explanation for this, but similar trends were observed in the M1 and M6 segments (*35*, *36*). Activation of CFTR in *Xenopus* oocytes appears to involve translocation of a cytoplasmic vesicle pool to the plasma membrane and the rate and extent of translocation depends on the magnitude of the CFTR conductance (*41*).

Effect of MTSES$^-$. Following activation, an 8-min application of 10 mM MTSES$^-$ to oocytes expressing wild-type CFTR had no effect on the CFTR-induced current (Figures 2A and 4). In contrast, a 1-min application of 10 mM MTSES$^-$ significantly inhibited the CFTR-induced currents for the mutants H199C, F200C, W202C, I203C, P205C, Q207C, and L211C (Figure 4). The extent of inhibition was similar after 1- and 8-min applications of MTSES$^-$, indicating that the reaction had gone to completion within 1 min (Figure 4). For the other cysteine-substitution mutants an 8-min application of MTSES$^-$ had no statistically significant effect on the CFTR-induced currents.

Effect of MTSEA$^+$. Application of 2.5 mM MTSEA$^+$ to oocytes expressing wild-type CFTR for up to 8 min had no effect on the CFTR-induced current (Figures 2C and 5). In contrast, a 1-min application of the positively charged reagent, 2.5 mM MTSEA$^+$, irreversibly inhibited the CFTR-induced currents of all of the cysteine-substitution mutants that reacted with MTSES$^-$ (Figure 2D and 5). In addition, a 1-min application of 2.5 mM MTSEA$^+$ also inhibited the mutant L214C (Figure 5). For all of the MTSEA$^+$ reactive mutants the extent of inhibition was similar after 1 and 8 min applications of MTSEA$^+$. This indicates that the reaction had gone to completion within 1 min. For the other cysteine-substitution mutants an 8-min application of MTSEA$^+$ had no statistically significant effect on the CFTR-induced currents.

Expression of the Δ259 CFTR Deletion Construct and Susceptibility to MTS Reagents. When expressed in *Xenopus* oocytes, a construct in which amino acids 1−259 have been deleted has been reported to yield functional channels (*39*). The structure of the conducting pathway in this deletion construct and its relationship to the structure of the conducting pathway of full-length CFTR is unknown. To probe the structure of the channel in the deletion construct, we tested the susceptibility of the Δ259-induced current to reaction with the MTS reagents. The mean conductance before addition of the cAMP-activating reagents was 0.4 ± 0.2 μS

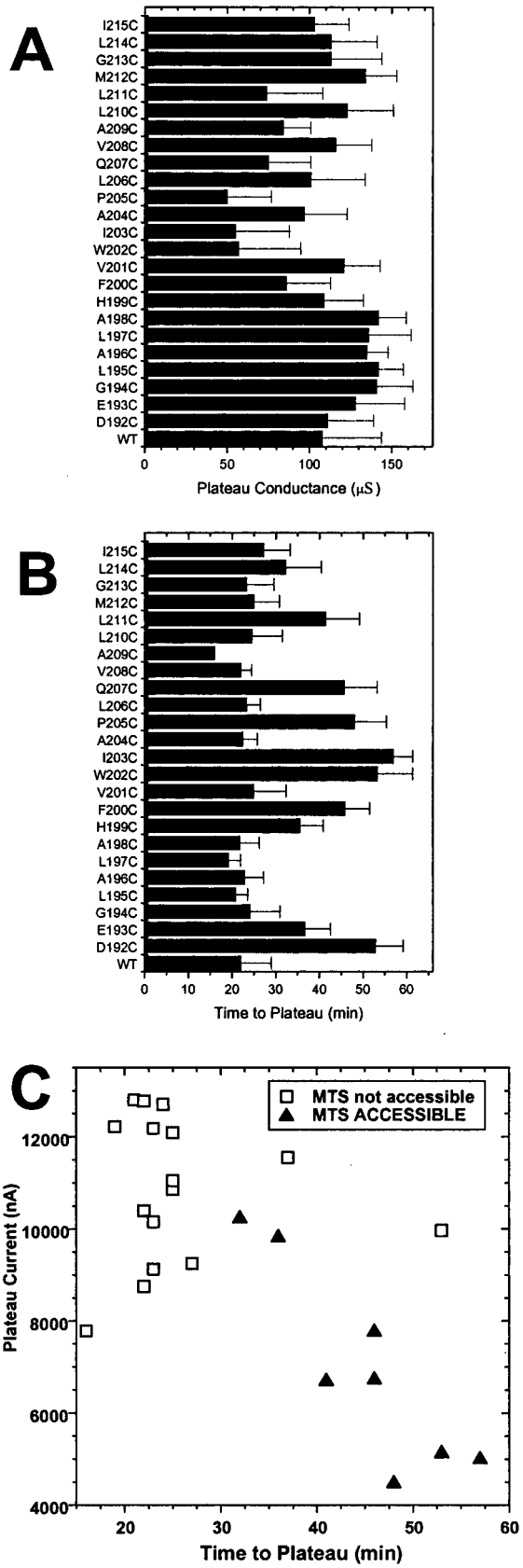

FIGURE 3: Plateau conductance and the time to reach the plateau conductance following the addition to the bath of the protein kinase A activating reagents for wild-type CFTR and the cysteine-substitution mutants. (A) Plateau conductance. (B) Time to reach the plateau conductance. (C) Plateau conductance plotted as a function of time to reach the plateau. (□) Residues that were not accessible to the MTS reagents. (▲) Residues that were accessible to the MTS reagents.

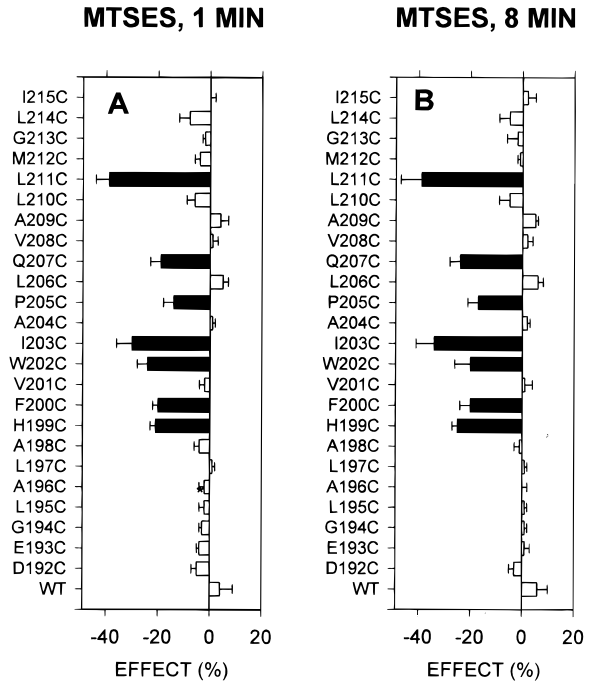

FIGURE 4: Effect of a 1- and 8-min application of 10 mM $MTSES^-$ on wild-type CFTR and the cysteine-substitution mutants. (A) Effect of a 1-min application. (B) Effect of an 8-min application. The solid bars indicate the effects that were significantly different from wild type by one-way ANOVA. Negative effects indicate inhibition; positive effect indicates potentiation of the subsequent current.

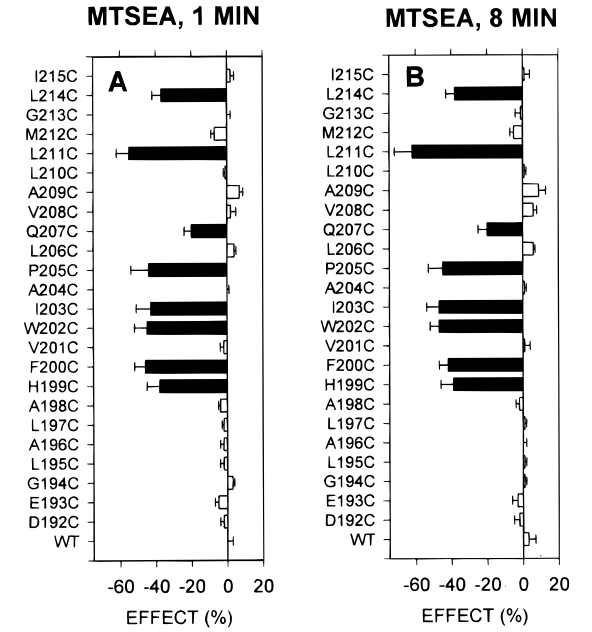

FIGURE 5: Effect of a 1- and 8-min application of 2.5 mM $MTSEA^+$ on wild-type CFTR and the cysteine-substitution mutants. (A) Effect of a 1-min application. (B) Effect of an 8-min application. The solid bars indicate the effects that were significantly different from wild type by one-way ANOVA. Negative effects indicate inhibition; positive effect indicates potentiation of the subsequent current.

($n = 7$). Following activation with the cAMP-activating reagents, the current reached a plateau in about 50 ± 5 min ($n = 7$). At the plateau the mean conductance was 53 ± 13 μS ($n = 7$).

As described above, an 8-min application of either 10 mM $MTSES^-$, 2.5 mM $MTSEA^+$, or 1 mM $MTSET^+$ (data not shown) to wild-type CFTR has no effect on the CFTR-induced current. In contrast, a 1-min application of 10 mM $MTSES^-$ irreversibly inhibited 33% ± 9% ($n = 2$) of the Δ259-induced current (Figure 6A). A 1-min application of 2.5 mM $MTSEA^+$ inhibited 75% ± 4% ($n = 3$) of the Δ259-induced current, and a 1-min application of 1 mM $MTSET^+$ inhibited 28% ± 8% ($n = 2$) of the Δ259-induced current (Figure 6 B,C). Thus, in contrast to wild-type CFTR, one or more of the endogenous cysteines in the Δ259 construct is accessible to react with the MTS reagents applied extracellularly.

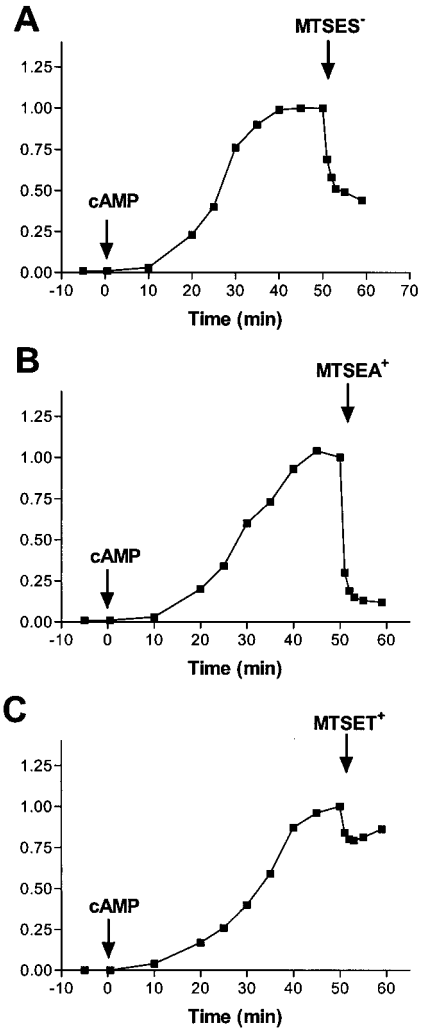

FIGURE 6: MTS reagents inhibit the current induced by the Δ259 deletion construct in *Xenopus* oocytes. Normalized current at −100 mV was recorded from individual oocytes expressing the deletion construct Δ259, which lacks the first 259 amino acids of CFTR. At the arrows marked cAMP, forskolin, IBMX, and cpt-cAMP were added to the bath. At the other arrow, (A) 10 mM $MTSES^-$, (B) 2.5 mM $MTSEA^+$, and (C) 1 mM $MTSET^+$ were added to the bath in the continued presence of the protein kinase A activating reagents. The currents were normalized to the value immediately preceding the addition of the MTS reagent: (A) 6855 nA, (B) 5225 nA, and (C) 5420 nA.

DISCUSSION

Identification of Water-Exposed Residues in the M3 Segment. The CFTR-induced currents of eight of the 24 cysteine-substitution mutants in the M3 segment were irreversibly altered by extracellular application of the charged, sulfhydryl-specific MTS reagents. We infer from the irreversible alteration of the CFTR-induced current that the

MTS reagents reacted with the engineered cysteines of these mutants. We assume that these reagents will only react with sulfhydryls that are on the water-accessible surface of the protein because the rate of reaction of the MTS reagents with an ionized thiolate anion (RS^-) is 5×10^9 times faster than the rate of reaction with the un-ionized thiol (RSH) (*42*); only sulfhydryls exposed to water will ionize to a significant extent. Furthermore, in a protein of known crystal structure, the extracellular domain of the aspartate chemotaxis receptor, the extent of reaction of a sulfhydryl reagent with engineered cysteines directly correlated with the surface accessibility of the corresponding wild-type residue (*37*). Thus, we assume that engineered cysteine residues that react with the MTS reagents are on the water-accessible surface of the protein. Therefore, for those cysteine-substitution mutants that reacted with the MTS reagents, we infer that the corresponding wild-type residues His199, Phe200, Trp202, Ile203, Pro205, Gln207, Leu211, and Leu214 are on the water-accessible surface of the protein.

On the basis of the assumption that the M3 segment spans the membrane, we assume that these residues form part of the channel lining. An alternative possibility is that these residues line a water-filled crevice that extends into the interior of the membrane-spanning domain but is not the channel. We think that this is unlikely for several reasons. Using the substituted-cysteine-accessibility method, we have demonstrated that a subset of the residues in the M1 and M6 membrane-spanning segments are also on the water-accessible surface of CFTR (*35, 36*). Thus, to date, at least three of the 12 putative membrane-spanning segments contain water-accessible faces. While the number of membrane-spanning segments that line the channel is unknown, given the diameter inferred from recent experiments (*43*) a minimum of five to six membrane-spanning segments would be needed to line the channel. Furthermore, a water-filled crevice other than the channel or transport pathway has not been observed in the three-dimensional structures of integral membrane proteins for which high-resolution structures are available (*44*−*51*). Thus, it is likely that these water-accessible faces of the M1, M3, and M6 segments line the channel.

The MTS reagents would fit into a right cylinder 6 Å in diameter and 10 Å in length. Thus, in order for the MTS reagents to reach the most cytoplasmic accessible residue in the M3 segment, H199C, the channel must be at least 6 Å in diameter from the extracellular end to the level of His199. We think that the channel diameter may be significantly larger than 6 Å over much of its length because modification of channel-lining cysteines, which adds a sphere that is roughly 6 Å diameter onto the cysteine, does not completely block conduction through the channel; in fact, the inhibition of current is generally less than 50%. A channel diameter greater than 6 Å is consistent with recent estimates of channel diameter based on the size of permeant anions (*43*).

It is tempting to assume that the residues for which the sulfhydryl reagents had no effect are not exposed in the channel lumen. Although this is the likely explanation, it may not be correct in all cases. We have measured the effects of modification using macroscopic currents; thus, it is possible that modification might increase open probability but decrease single-channel conductance or *vice versa*, resulting in an unaltered macroscopic current. Alternatively,

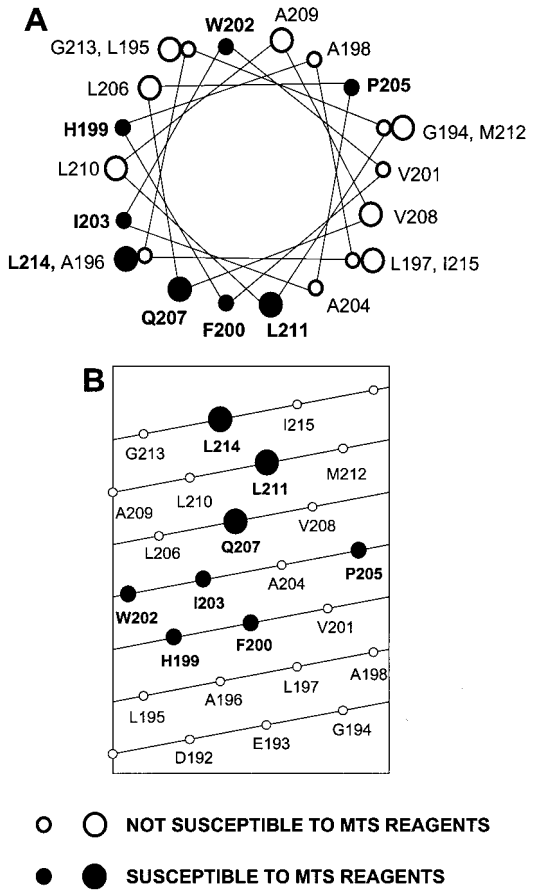

FIGURE 7: α-Helical representations of the residues in and flanking the M3 membrane-spanning segment. (A) α-Helical wheel representation. (B) α-Helical net representation. Extracellular is at the top, intracellular is at the bottom. The *x*-axis represents the circumference of the helix; residues that are aligned vertically are on the same face of the helix. (●) MTS-accessible residues more extracellular than Pro205; (●) MTS-accessible residues at or more cytoplasmic to Pro205. In panel A: (○) residues more extracellular than Pro205 that do not react with the MTS reagents; (○) residues at or more cytoplasmic to Pro205 that do not react with the MTS reagents.

local steric constraints may prevent access of the reagents to an engineered cysteine residue in the channel-lining. Finally, as with any experiment using site-directed mutagenesis, the mutation may alter the protein structure so that the accessibility of the engineered cysteine does not accurately reflect the accessibility of the corresponding wild-type residue.

Secondary Structure of the M3 Segment. On the basis of the periodicity of the channel-lining residues, we can infer the secondary structure of the M3 segment. The periodicity of the accessible residues is not consistent with a β-strand secondary structure. When the residues in the extracellular half of the segment from Gln207−Leu214 are plotted on an α-helical wheel, the accessible residues lie on one face of the helix within an arc of 60° (Figure 7). When the residues more cytoplasmic than Pro205 are plotted on an α-helical wheel, the accessible residues lie within an arc of 160° and appear to form two turns of an α-helix. Thus, the M3 segment appears to be largely α-helical except in the region of Pro205. Thomas and co-workers determined that the secondary structure of a synthetic peptide with the M3 segment sequence was largely α-helical in membrane-mimetic environments (*33*). Interestingly, the UV absor-

bance spectra of the M3 peptide contained a large absorbance shoulder at 228 nm characteristic of a ring−charge interaction (*33*, *52*). If His199 were protonated this ring-charge interaction could result from an interaction of His199 and Trp202, which are separated by one helical turn on the water-accessible face of the helix.

Pro205, in the middle of the M3 segment, appears to induce a bend or kink in the helix. The arc encompassed by the exposed face of the cytoplasmic half of the M3 segment is much greater than the extracellular half (160° vs 60°) (Figure 7). The bend induced by Pro205 may cause the cytoplasmic end of M3 to angle away from the channel wall in toward the central axis of the channel. Such a bend could explain the larger exposed surface in the cytoplasmic half of M3. A similar proline-induced bend has been observed in the M7 membrane-spanning segment of the dopamine D2 receptor (*53*). The proline-induced bend in M3 could serve to narrow the channel at its cytoplasmic end. To explain the observed voltage dependence of the rates of reaction of charged sulfhydryl reagents with channel-lining cysteines in the M6 segment, we previously suggested that the channel narrowed at its cytoplasmic end (*54*).

Proline residues are often considered to disrupt α-helical secondary structure; however, in membrane-mimetic environments proline can exist in α-helical domains (*55*, *56*). Interestingly, prolines are found in about 20% of putative transmembrane helices but in only 3% of helices in globular proteins (*57*). The mutation P205S is associated with mild CF (*58*); this and other mutations of Pro205 reduce the formation of mature CFTR protein but they do not alter the halide permeability and conductance ratios (*31*). Although mutations of Pro205 may reduce the efficiency of assembly, they may not significantly alter the secondary structure of the M3 segment because other packing constraints may be sufficient to maintain the bend. This has been observed in the structure of the photosynthetic reaction center. There is a proline-kinked helix in the L subunit. In the homologous M subunit an alanine occurs at the aligned position, yet the helix is kinked in a manner similar to the L subunit helix (*57*).

As a consequence of Pro205 the normal α-helical H-bond donor for the carbonyl of Val201 is absent. In addition, the H-bond between Leu206 and Trp202 will be disrupted by the proline bend (*57*). Thus, several backbone carbonyls and amides are potentially available to interact with ions in the channel; however, the role of such potential interactions in the CFTR channel is unknown. Interactions between backbone carbonyls and potassium ions were inferred from the crystal structure of a potassium channel (*48*).

Although the 16 residues from His199−Leu214 are shorter than a typical membrane-spanning segment of 20 residues, the proline bend may effectively lengthen the helix, allowing it to span the membrane (*57*, *59*). Alternatively, additional residues near the cytoplasmic end of the M3 segment may be exposed in the channel but local steric factors may reduce the ability of the MTS reagents to react with cysteines substituted for these residues.

Structure of the Channel in the Deletion Construct Δ259. A deletion construct, Δ259, that eliminates the M1−M4 membrane-spanning segments is reported to induce a current in *Xenopus* oocytes that is similar to that for CFTR (*39*). On this basis, it has been suggested that the M1−M4 segments may not be involved in forming the channel of wild-type CFTR. The question arises as to what is the structure of the ion channel of Δ259, and is that structure similar to the chloride channel structure of full-length CFTR? To begin to address this issue, we probed the sensitivity of the Δ259-induced current to modification by sulfhydryl-reactive reagents. In contrast to full-length CFTR, the current induced by the Δ259 construct is inhibited by the MTS reagents (Figure 6). This implies that at least one of the 15 endogenous cysteines in the Δ259 construct is on the water-accessible surface of the protein and is accessible from the extracellular bath.[2] In the Δ259 construct, two cysteines remain in membrane-spanning segments, Cys343 (M6) and Cys866 (M7), and 13 remain in putative cytoplasmic domains. The accessibility from the extracellular bath of at least one cysteine in the Δ259 construct implies that the arrangement of the membrane-spanning segments in the Δ259 construct is different from their arrangement in full-length CFTR. Thus, while some of the functional properties of the Δ259 construct may be similar to those of full-length CFTR, its structure is different. On the basis of our previous work and the current results, we believe that residues from the M1, M3, and M6 membrane-spanning segments are on the water-accessible surface of the channel formed by wild-type CFTR (*35*, *36*).

Relationship to Other Work on CFTR. Several mutations of residues in and flanking the M3 membrane-spanning segment have been identified in patients with CF, including D192G, E193K, H199Y, P205S, and L206W (*58*, *60*−*63*). Thus, mutation of both channel-lining and buried residues can cause CF. Understanding the structural basis by which these mutations alter the function of the protein will require a more detailed structure of the channel that is slowly emerging.

[2] This assumes that the current is passing through a channel formed by the Δ259 construct. Alternatively, the Δ259 construct may cause another protein to move to the plasma membrane or activate another protein in the plasma membrane that forms the ion conducting pathway.

ACKNOWLEDGMENT

We thank Ms. Rong Schick for expert technical assistance and Drs. Jonathan Javitch and Arthur Karlin for helpful discussions and comments on the manuscript.

REFERENCES

1. Riordan, J. R., Rommens, J. M., Kerem, B. S., Alon, N., Rozmahel, R., Grzelczak, Z., Zielenski, J., Lok, S., Plavsic, N., Chou, J. L., Drumm, M. T., Iannuzzi, M. C., Collins, F. S., and Tsui, L. C. (1989) *Science 254*, 1066−1073.
2. Riordan, J. R. (1993) *Annu. Rev. Physiol. 55*, 609−630.
3. Gadsby, D. C., Nagel, G., and Hwang, T.-C. (1995) *Annu. Rev. Physiol. 57*, 387−416.
4. Egan, M., Flotte, T., Afione, S., Solow, R., Zeitlin, P. L., Carter, B. J., and Guggino, W. B. (1992) *Nature 358*, 581−584.
5. Gabriel, S. E., Clarke, L. C., Boucher, R. C., and Stutts, M. J. (1993) *Nature 363*, 263−266.
6. Schwiebert, E. M., Egan, M. E., Hwang, T. H., Fulmer, S. B., Allen, S. A., Cutting, G. R., and Guggino, W. B. (1995) *Cell 81*, 1063−1073.
7. Stutts, M. J., Canessa, C. M., Olsen, J. C., Hamrick, M., Cohn, J. A., Rossier, B. C., and Boucher, R. C. (1995) *Science 269*, 847−850.

8. Sugita, M., Yue, Y., and Foskett, J. K. (1998) *EMBO J. 17*, 898−908.
9. Field, M., and Semrad, C. E. (1993) *Annu. Rev. Physiol. 55*, 631−655.
10. Vaandrager, A. B., Smolenski, A., Tilly, B. C., Houtsmuller, A. B., Ehlert, E. M., Bot, A. G., Edixhoven, M., Boomaars, W. E., Lohmann, S. M., and de Jonge, H. R. (1998) *Proc. Natl. Acad. Sci. U.S.A. 95*, 1466−1471.
11. Hanrahan, J. W., Mathews, C. J., Grygorczyk, R., Tabcharani, J. A., Grzelczak, Z., Chang, X. B., and Riordan, J. R. (1996) *J. Exp. Zool. 275*, 283−291.
12. Tabcharani, J. A., Chang, X. B., Riordan, J. R., and Hanrahan, J. W. (1991) *Nature 352*, 628−631.
13. Chang, X.-B., Tabcharani, J. A., Hou, Y.-X., Jensen, T. J., Kartner, N., Alon, N., Hanrahan, J. W., and Riordan, J. R. (1993) *J. Biol. Chem. 268*, 11304−11311.
14. Jia, Y., Mathews, C. J., and Hanrahan, J. W. (1997) *J. Biol. Chem. 272*, 4978−4984.
15. Seibert, F. S., Tabcharani, J. A., Chang, X. B., Dulhanty, A. M., Mathews, C., Hanrahan, J. W., and Riordan, J. R. (1995) *J. Biol. Chem. 270*, 2158−2162.
16. Mathews, C. J., Tabcharani, J. A., Chang, X. B., Jensen, T. J., Riordan, J. R., and Hanrahan, J. W. (1998) *J. Physiol. (London) 508*, 365−377.
17. Anderson, M. P., Berger, H. A., Rich, D. P., Gregory, R. J., Smith, A. E., and Welsh, M. J. (1991) *Cell 67*, 775−784.
18. Gunderson, K. L., and Kopito, R. R. (1995) *Cell 82*, 231−239.
19. Winter, M. C., Sheppard, D. N., Carson, M. R., and Welsh, M. J. (1994) *Biophys. J. 66*, 1398−1403.
20. Schultz, B. D., Bridges, R. J., and Frizzell, R. A. (1996) *J. Membr. Biol. 151*, 63−75.
21. Denning, G. M., Ostedgaard, L. S., and Welsh, M. J. (1992) *J. Cell Biol. 118*, 551−559.
22. Schultz, B. D., Takahashi, A., Liu, C., Frizzell, R. A., and Howard, M. (1997) *Am. J. Physiol. 273*, C2080−C2089.
23. Chang, X. B., Hou, Y. X., Jensen, T. J., and Riordan, J. R. (1994) *J. Biol. Chem. 269*, 18572−18575.
24. Baukrowitz, T., Hwang, T.-C., Nairn, A. C., and Gadsby, D. C. (1994) *Neuron 12*, 473−482.
25. Cheng, S. H., Rich, D. P., Marshall, J., Gregory, R. J., Welsh, M. J., and Smith, A. E. (1991) *Cell 66*, 1027−1036.
26. Hwang, T. C., Horie, M., and Gadsby, D. C. (1993) *J. Gen. Physiol. 101*, 629−650.
27. Anderson, M. P., Gregory, R. J., Thompson, S., Souza, D. W., Paul, S., Mulligan, R. C., Smith, A. E., and Welsh, M. J. (1991) *Science 253*, 202−205.
28. Tabcharani, J. A., Rommens, J. M., Hou, Y. X., Chang, X. B., Tsui, L. C., Riordan, J. R., and Hanrahan, J. W. (1993) *Nature 366*, 79−82.
29. McDonough, S., Davidson, N., Lester, H. A., and McCarty, N. A. (1994) *Neuron 13*, 623−634.
30. Sheppard, D. N., Rich, D. P., Ostedgaard, L. S., Gregory, R. J., Smith, A. E., and Welsh, M. J. (1993) *Nature 362*, 160−164.
31. Sheppard, D. N., Travis, S. M., Ishihara, H., and Welsh, M. J. (1996) *J. Biol. Chem. 271*, 14995−15001.
32. Ostedgaard, L. S., Rich, D. P., DeBerg, L. G., and Welsh, M. J. (1997) *Biochemistry 36*, 1287−1294.
33. Wigley, W. C., Vijayakumar, S., Jones, J. D., Slaughter, C., and Thomas, P. J. (1998) *Biochemistry 37*, 844−853.
34. Akabas, M. H., Stauffer, D. A., Xu, M., and Karlin, A. (1992) *Science 258*, 307−310.
35. Akabas, M. H., Kaufmann, C., Cook, T. A., and Archdeacon, P. (1994) *J. Biol. Chem. 269*, 14865−14868.
36. Cheung, M., and Akabas, M. H. (1996) *Biophys. J. 70*, 2688−2695.
37. Danielson, M. A., Bass, R. B., and Falke, J. J. (1997) *J. Biol. Chem. 272*, 32878−32888.
38. Cotten, J. F., and Welsh, M. J. (1997) *J. Biol. Chem. 272*, 25617−25622.
39. Carroll, T. P., Morales, M. M., Fulmer, S. B., Allen, S. S., Flotte, T. R., Cutting, G. R., and Guggino, W. B. (1995) *J. Biol. Chem. 270*, 11941−11946.
40. Stauffer, D. A., and Karlin, A. (1994) *Biochemistry 33*, 6840−6849.
41. Takahashi, A., Watkins, S. C., Howard, M., and Frizzell, R. A. (1996) *Am. J. Physiol. 271*, C1887−C1894.
42. Roberts, D. D., Lewis, S. D., Ballou, D. P., Olson, S. T., and Shafer, J. A. (1986) *Biochemistry 25*, 5595−5601.
43. Linsdell, P., and Hanrahan, J. W. (1998) *J. Gen. Physiol. 111*, 601−614.
44. Deisenhofer, J., Epp, O., Miki, K., Huber, R., and Michel, H. (1985) *Nature 318*, 618−624.
45. Cowan, S. W., Schirmer, T., Rummel, G., Steiert, M., Ghosh, R., Pauptit, R. A., Jansonius, J. N., and Rosenbusch, J. P. (1992) *Nature 358*, 727−733.
46. Schirmer, T., Keller, T. A., Wang, Y.-F., and Rosenbusch, J. P. (1995) *Nature 267*, 512−514.
47. Weiss, M. S., Abele, U., Weckesser, J., Welte, W., Schiltz, E., and Schulz, G. E. (1991) *Science 254*, 1627−1630.
48. Doyle, D. A., Cabral, J. M., Pfuetzner, R. A., Kuo, A., Gulbis, J. M., Cohen, S. L., Chait, B. T., and MacKinnon, R. (1998) *Science 280*, 69−77.
49. Tsukihara, T., Aoyama, H., Yamashita, E., Tomizaki, T., Yamaguchi, H., Shinzawa-Itoh, K., Nakashima, R., Yaono, R., and Yoshikawa, S. (1996) *Science 272*, 1136−1144.
50. Koepke, J., Hu, X., Muenke, C., Schulten, K., and Michel, H. (1996) *Structure 4*, 581−597.
51. Kuhlbrandt, W. (1995) *Structure 3*, 521−525.
52. Clark, P. L., Liu, Z. P., Zhang, J., and Gierasch, L. M. (1996) *Protein Sci. 5*, 1108−1117.
53. Fu, D., Ballesteros, J. A., Weinstein, H., Chen, J., and Javitch, J. A. (1996) *Biochemistry 35*, 11278−11285.
54. Cheung, M., and Akabas, M. H. (1997) *J. Gen. Physiol. 109*, 289−300.
55. Li, S. C., and Deber, C. M. (1994) *Nat. Struct. Biol. 1*, 368−373.
56. Li, S. C., Goto, N. K., Williams, K. A., and Deber, C. M. (1996) *Proc. Natl. Acad. Sci. U.S.A. 93*, 6676−6681.
57. von Heijne, G. (1991) *J. Mol. Biol. 218*, 499−503.
58. Chillon, M., Casals, T., Nunes, V., Gimenez, J., Perez Ruiz, E., and Estivill, X. (1993) *Hum. Mol. Genet. 2*, 1741−1742.
59. Ballesteros, J. A., and Weinstein, H. (1992) *Biophys. J. 62*, 110−111.
60. Audrezet, M. P., Canki-Klain, N., Mercier, B., Bracar, D., Verlingue, C., and Ferec, C. (1994) *Hum. Genet. 93*, 659−662.
61. Mercier, B., Verlingue, C., Lissens, W., Silber, S. J., Novelli, G., Bonduelle, M., Audrezet, M. P., and Ferec, C. (1995) *Am. J. Hum. Genet. 56*, 272−277.
62. Claustres, M., Laussel, M., Desgeorges, M., Giansily, M., Culard, J. F., Razakatsara, G., and Demaille, J. (1993) *Hum. Mol. Genet. 2*, 1209−1213.
63. Morral, N., Dork, T., Llevadot, R., Dziadek, V., Mercier, B., Ferec, C., Costes, B., Girodon, E., Zielenski, J., Tsui, L. C., Tummler, B., and Estivill, X. (1996) *Hum. Mutat. 8*, 149−159.

BI980969O